

Admittance Control for Physical Human-Quadrocopter Interaction

Federico Augugliaro and Raffaello D'Andrea

Abstract—This paper analyzes the application of admittance control to quadrocopters, focusing on physical human-vehicle interaction. Admittance control allows users to define the apparent inertia, damping, and stiffness of a robot, providing an intuitive way to physically interact with it. In this work, external forces acting on the quadrocopter are estimated from position and attitude information and then input to the admittance controller, which modifies the vehicle reference trajectory accordingly. The reference trajectory is tracked by an underlying position and attitude controller. The characteristics of the overall control scheme are investigated for the near-hover case. Experimental results complement the paper, demonstrating the suitability of the method for physical human-quadrocopter interaction.

I. INTRODUCTION

In the last decade, quadrocopters have been a popular platform for unmanned aerial vehicle (UAV) research. High-accuracy flight still relies on external localization methods, but advances in sensor capabilities and their growing miniaturization has drastically improved the possibility of on-board perception and state estimation, allowing, for example, autonomous flight using onboard processing for computer vision [1]. Recent progress in vehicle design, such as lighter components and improved propeller design, have enabled higher lift capabilities, longer autonomy and higher thrust-to-power ratios. Today, quadrocopters offer an excellent compromise between payload capability, agility and robustness [2].

Hover-capable UAVs, however, were mostly seen as sensing robots, particularly useful in tasks like search and rescue, surveillance and inspection. Interaction with the environment was not investigated until recently, when some groups started exploring the possibility of carrying objects with autonomous hover-capable UAVs. Various strategies for multiple UAVs cooperating to lift payloads are presented in [3]–[6]. In [7], the closed-loop stability of helicopters and quadrocopters carrying payloads is analyzed. The past year has seen an impressive increase in published work in the context of aerial manipulation. The AIRobots project [8] addresses the inspection of the environment by contact. Hybrid position-force control methods are presented for ducted-fan vehicles [9] and quadrocopters [10] in contact with the environment, whereas impedance control for an aerial manipulator is investigated in [11]. The ARCAS project [12] focuses on aerial assembly by helicopters equipped with robotic arms. Modeling and control of an aerial manipulator is also treated in [13]. In this context, we demonstrated the ability of quadrocopters to

erect structures by assembling a 6 meter tower out of 1500 foam bricks [14].

Unforeseen behaviours can occur when aerial vehicles interact with their environment, potentially leading to unstable or dangerous situations that can harm people, damage the surroundings, or damage the vehicle itself. Based in the Flying Machine Arena [16], a testbed for quadrocopter research at ETH Zurich, our research addresses the need for UAVs to safely and appropriately handle physical interaction with their environment. In the following sections, we analyze the application of impedance control to quadrocopters, and present a near-hover analysis of the system and experimental results that focus on human-vehicle interaction (Figure 1). Impedance control is a well-known control scheme that regulates the mechanical impedance of a robot in contact with the environment through force feedback [17], [18], and is commonly used for robotic arms. It allows users to modify the apparent inertia, damping, and stiffness of the robot as needed: For example, a robot can be modeled in such a way that a human physically interacting with it perceives a low mass object subject to damping. We take advantage of the underlying control scheme developed at the Flying Machine Arena [19], and we add an outer control loop that modifies the reference trajectory, which is input to a position controller, according to an estimate of the external forces acting on the quadrocopter, as outlined in Figure 3. This strategy is called admittance control, see for example [20]. Adding an outer control loop that simply

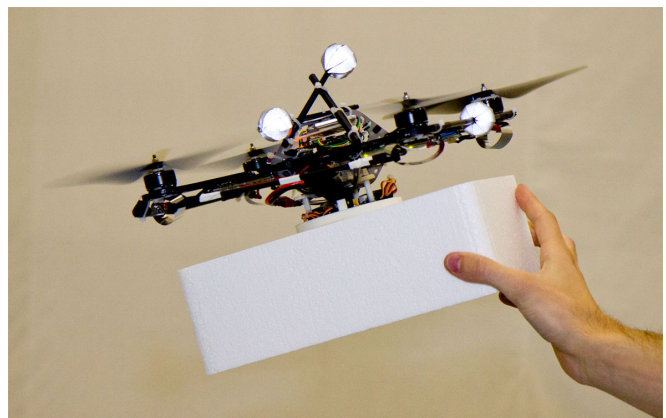


Fig. 1. Human-quadrocopter interaction: Admittance control provides an intuitive way to physically interact with quadrocopters. In the picture, a quadrocopter carrying a foam brick is physically guided by the user. The vehicle is equipped with soft propellers that do not seriously harm the user in the event of accidental contact. To improve safety, the vehicle could be enclosed by a protective cage, such as the Qball-X4 [15].

The authors are with the Institute for Dynamic Systems and Control, ETH Zurich, Switzerland. {faugugliaro, rdandrea}@ethz.ch

modifies the reference position enables the use of a well-tuned, thoroughly tested underlying controller, and permits a smooth switch between force and position control, with the admittance controller acting as a simple pass-through in the latter case.

Hybrid force-position control strategies are often used in assembly tasks with robotic manipulators, such as the peg-in-hole problem. Generally speaking, admittance control (or other force control approaches) is used whenever compliance with the environment is necessary. While both tasks are of interest to aerial robots, in this work we present a different application of admittance control to quadcopters: We explore the possibility of physical human-vehicle interaction. Physical human-robot interaction has been largely treated in the context of humanoid/mobile robots, however, physical interaction between a person and a UAV has seen little research activity (an example can be found in [21]). Reliable and safe physical interaction with UAVs will be of great importance in real world applications, where robots will tightly cooperate with humans, such as, for example, on a construction site [22].

The paper is organized as follows: In Section II, we present the overall control strategy and the method used to estimate the forces acting on a quadcopter using position and attitude information only. Section III contains a near-hover analysis of the system. In Section IV, we present a scenario in which quadcopters can benefit from admittance control: physical human-vehicle interaction. Experimental results are included.

II. CONTROL STRATEGY

In this section we present a qualitative description of the overall control strategy used in this work. We provide a three-dimensional model of the quadcopter, an overview of the controller scheme used in the Flying Machine Arena, the definition of admittance controller, and we present the method used to estimate the unknown external forces acting on the vehicle from position and attitude information. A detailed mathematical description of the control and estimation strategies for the near-hover case can be found in Section III.

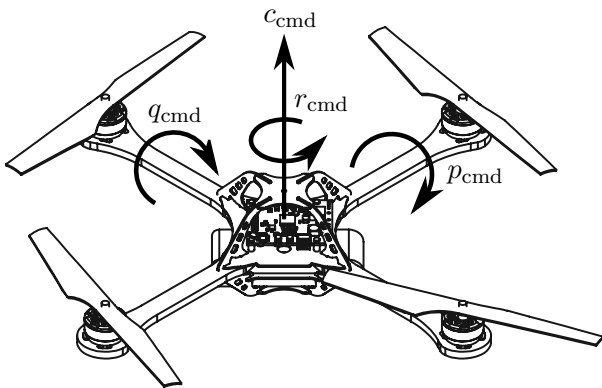


Fig. 2. A drawing of the quadcopters used in the Flying Machine Arena. The arrows represent the four control inputs: the collective thrust c_{cmd} , and the rotational body rates p_{cmd} , q_{cmd} , and r_{cmd} .

The equations presented in this work refer to continuous-time systems. We omit the time dependency to ease readability.

A. Quadcopter model

We model the quadcopter (Figure 2) from first principles as a rigid body, neglecting aerodynamic effects. This model has been experimentally proven to provide good performance, with unmodeled aerodynamic effects becoming relevant only at high speed [23]. The mass-normalized translational dynamics of a quadcopter in the inertial frame are modeled as

$$\begin{bmatrix} \ddot{x} \\ \ddot{y} \\ \ddot{z} \end{bmatrix} = R \begin{bmatrix} 0 \\ 0 \\ c \end{bmatrix} - \begin{bmatrix} 0 \\ 0 \\ g \end{bmatrix}, \quad (1)$$

where R represents the rotation matrix from the body frame (which is fixed on the quadcopter) to the inertial frame, c is the collective thrust generated by the four propellers, and g is the gravitational acceleration. The rotation matrix R evolves according to

$$\dot{R} = R \begin{bmatrix} 0 & -r & q \\ r & 0 & -p \\ -q & p & 0 \end{bmatrix}, \quad (2)$$

where $\omega = (p, q, r)$ represents the rotational body rates around the body axes. The quadcopter is controlled by four inputs: a collective thrust command c_{cmd} , and commanded rotational body rates p_{cmd} , q_{cmd} , and r_{cmd} .

B. Quadcopter control strategy

The strategy used in the Flying Machine Arena to control the quadcopters consists of cascaded control loops governing altitude, horizontal translation, and attitude.

The controller accepts as input a reference trajectory $\Lambda_r = (x_r, y_r, z_r)$ and, based on the current state estimate, computes the four necessary control inputs that are sent to the quadcopter. Onboard, an additional control loop appropriately tracks the commanded collective thrust and rotational rates by controlling the motor forces. We do not provide a full description of the control scheme. Instead, in Section III we present a near-hover analysis of the overall control architecture to evaluate its characteristics. For more details on the controller used in the Flying Machine Arena we refer the reader to [19].

C. Admittance controller

The controller scheme currently in use in the Flying Machine Arena does not explicitly address the effect of external forces acting on the quadcopter: These are simply treated as disturbances. With this work, we take into account these external forces by adding an outer control loop that modifies the reference trajectory Λ_r that is input to the position controller accordingly. The user can also specify a desired trajectory $\Lambda_d = (x_d, y_d, z_d)$. The dynamic behaviour of the reference trajectory Λ_r is then captured by the following mass-spring-damper system:

$$M(\ddot{\Lambda}_d - \ddot{\Lambda}_r) + D(\dot{\Lambda}_d - \dot{\Lambda}_r) + K(\Lambda_d - \Lambda_r) = -f, \quad (3)$$

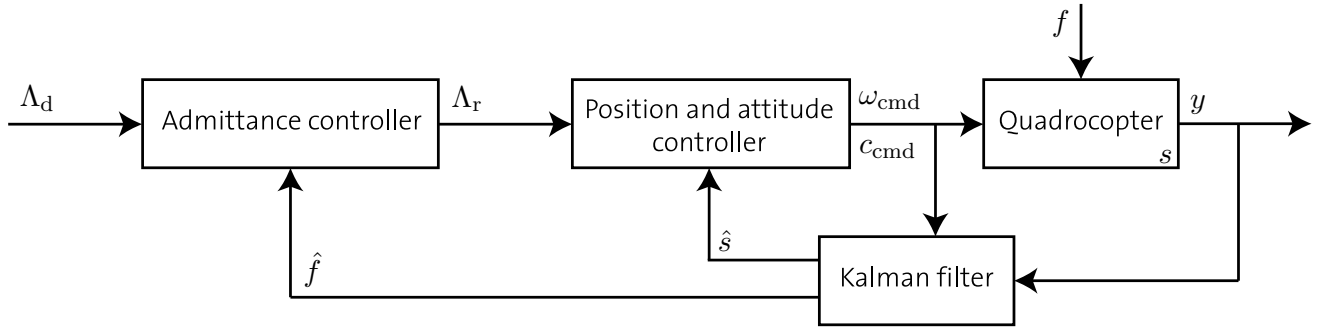


Fig. 3. The overall control strategy. User input to the system is the desired trajectory Λ_d . Furthermore the quadcopter is subject to external forces f . The admittance controller modifies the reference trajectory Λ_r that is input to the position controller according to an estimate of the external forces \hat{f} . The collective thrust c_{cmd} and the rotational body rates ω_{cmd} are the control inputs to the quadcopter. Its state is given by s . The measurement vector y contains position and attitude.

where f are the external forces acting on the vehicle. The diagonal matrices M , D , and K define the apparent inertia, damping, and stiffness of the vehicle. This means that, assuming perfect reference tracking, if the vehicle is pushed or pulled it will behave according to (3). During a human-vehicle interaction situation, we want the user to be able to physically guide the quadcopter in space; we thus pick $K = 0$ and $\dot{\Lambda}_d = \ddot{\Lambda}_d = 0$. The general framework (3) is used when both trajectory tracking and compliance with the environment are required.

D. Force estimation

The control strategy presented above assumes that the external forces acting on the vehicle are known. When the exact contact point of the robot-environment interaction is known, such as in grasping tasks, a force sensor can provide the required information. If, however, the interaction can be performed anywhere on the quadcopter, other means of obtaining these forces are necessary. As already suggested in [10] for the case of quasistatic motion, we rely only on position and attitude information to estimate the external forces acting on the vehicle. We use a simple approach based on the unscented Kalman filter [24] to estimate the quadcopter state and the external forces and torques acting on it.

1) *States*: The state vector consists of 18 states: Position and velocity of the vehicle, rotational body rates, attitude representation, and forces and torques acting on the quadcopter.

2) *Process model*: The dynamics (1) and (2) are extended in order to capture the external forces acting on the vehicle. Furthermore, non-idealities such as the quadcopter response to the commanded inputs are taken into account. Since the model of the external forces acting on the vehicle is not known, we assume that the change of external forces and torques is purely driven by noise, with the noise values being tuning parameters of the filter. The system is assumed to be subject to angular and translational acceleration additive zero-mean process noise.

3) *Measurement model*: The quadcopter position and attitude are directly observed by an external motion capture

system. We assume that the data is subject to additive zero-mean measurement noise. The model presented here is applicable to any localization method that provides position and attitude information.

III. NEAR-HOVER ANALYSIS

In order to analyze the system behaviour and stability, we present a near-hover analysis of the closed-loop system described in Section II (and depicted in Figure 3) along one translational direction. The same considerations apply to the other directions as well. We assume that the altitude of the vehicle is kept constant by the feed-forward mass-normalized collective thrust command $c_{\text{cmd}} = g$. We consider the translational dynamics along x and the rotation about the pitch angle θ . The propellers produce a torque τ that acts on the positive θ direction. In the following, we fully describe the subsystems that compose the overall system.

A. Quadcopter

The state vector is given by $s = (x, \dot{x}, \theta, \dot{\theta}, \tau)$, the control input $u = \dot{\theta}_{\text{cmd}}$ is the commanded body rotational rate, and f_x represents an external force acting on the vehicle in the positive x direction. Here, we assume zero external torque. Following the notation of [25], we denote zero-mean continuous-time white noise with covariance $Q\delta(t)$ as $w \sim (0, Q)$. The vectors $w \sim (0, Q)$ and $v \sim (0, R)$ represent the additive process noise and measurement noise, respectively.

The lateral dynamics of the quadcopter about hover are captured by

$$\ddot{x} = g\theta + \frac{f_x}{m} + w_2, \quad (4)$$

where m is the vehicle's mass and $w_2 \sim (0, Q_2)$ affects the lateral acceleration and represents the second element of the process noise vector w .

The rotational dynamics of the vehicle are given by

$$\ddot{\theta} = \frac{\tau}{I} + w_4, \quad (5)$$

where I is the moment of inertia and $w_4 \sim (0, Q_4)$ represents the process noise acting on the rotational acceleration. Experiments have shown that the torque generated by the

vehicle responds to the commanded torque τ_{cmd} as a first-order system with time constant T_1 , thus resulting in

$$\dot{\tau} = \frac{1}{T_1}(\tau_{\text{cmd}} - \tau). \quad (6)$$

With the desired angular rate $\dot{\theta}_{\text{cmd}}$ sent to the quadcopter, the onboard control loop computes the torque τ_{cmd} necessary to track the command using the onboard rate gyros. The onboard control loop is shaped such that the rotational rate reacts in the manner of a first-order system with time constant T_2 by

$$\tau_{\text{cmd}} = \frac{I}{T_2} (\dot{\theta}_{\text{cmd}} - \dot{\theta}). \quad (7)$$

Position and attitude of the quadcopter are known. The measurement vector is thus

$$y = (x, \theta). \quad (8)$$

Equations (4)-(8) can be written as

$$\begin{aligned} \dot{s} &= As + Bu + f_E + w, \\ y &= Cs + v, \end{aligned} \quad (9)$$

by appropriately defining the system matrices A , B , and C and the noise covariance diagonal matrices Q and R . The vector $f_E = (0, \frac{f_x}{m}, 0, 0, 0)$ contains the external force.

B. Position and attitude controller

The position controller accepts a reference position x_r as input and sends a commanded rotational rate $\dot{\theta}_{\text{cmd}}$ to the quadcopter. The control strategy is chosen such that the lateral dynamics (assuming no external force) behave as a second-order system with time constant T_4 and damping ratio ζ . From (4), we thus require

$$\theta_r = \frac{1}{g} \left(\frac{1}{T_4^2} (x_r - x) + \frac{2\zeta}{T_4} (-\dot{x}) \right), \quad (10)$$

such that, in the ideal case and with $f_x = 0$ we have

$$\ddot{x} + \frac{2\zeta}{T_4} \dot{x} + \frac{1}{T_4^2} x = \frac{1}{T_4^2} x_r. \quad (11)$$

The attitude controller is shaped such that the angle error behaves as a first-order system with time constant T_3 . The commanded angle rate $\dot{\theta}_{\text{cmd}}$ is thus

$$\dot{\theta}_{\text{cmd}} = \frac{1}{T_3} (\theta_r - \theta). \quad (12)$$

C. Kalman filter

We consider the linear system (9). Because the unscented Kalman filter approximates mean and covariance correctly to second order [24], the linear case reduces to the standard Kalman filter. In addition to the quadcopter state, we also estimate the external force acting on the vehicle. We thus choose the following augmented state s_K for the Kalman filter:

$$s_K = (s, f_x). \quad (13)$$

As stated above, we assume that the force is purely driven by noise. We thus have

$$\dot{f}_x = w_6, \quad (14)$$

with $w_6 \sim (0, Q_6)$. The covariance matrix Q is augmented accordingly, resulting in Q_K . For the purpose of our analysis we are interested in the steady-state Kalman filter (see, for example [25]). The augmented system is given by

$$\begin{aligned} \dot{s}_K &= A_K s_K + B_K u + w_K, \\ y_K &= C_K s_K + v, \end{aligned} \quad (15)$$

where A_K , B_K , C_K , and $w_K \sim (0, Q_K)$ can be derived from (9), (13), and (14). The state estimate \hat{s}_K evolves as

$$\dot{\hat{s}}_K = (A_K - L C_K) \hat{s}_K + L y + B_K u, \quad (16)$$

where we have

$$L = P C_K^T R^{-1}. \quad (17)$$

The positive-definite matrix P is the solution of the continuous-time algebraic Riccati equation

$$-P C_K^T R^{-1} C_K P + A_K P + P A_K^T + Q_K = 0. \quad (18)$$

D. Admittance controller

The underlying position and attitude controller has been appropriately tuned by loop-shaping techniques and is currently used in the Flying Machine Arena for everyday operations. It provides good trajectory tracking and disturbance rejection performance. In Section II-C, we presented the idea behind admittance control. From (3), and using the estimated external force \hat{f}_x and the desired trajectory x_d as input, we obtain the following mass-spring-damper system:

$$-M_x \ddot{x}_r - D_x \dot{x}_r + K_x (x_d - x_r) = -\hat{f}_x, \quad (19)$$

where M_x , D_x , and K_x are scalar values defining the dynamics of the reference trajectory x_r . As already mentioned, for human-vehicle interaction we pick $K_x = 0$.

E. Analysis and separated dynamics

The four subsystems described above define the closed-loop behaviour of the system near hover. Most of the time, in an interaction task, the vehicle is very close to the hover position. Therefore, the near-hover analysis provides us with good insight into the three-dimensional system: it is used to tune the controller parameters and to assess the stability of the system. Furthermore, the analysis shows that the dynamics of the admittance controller, the underlying position and attitude controller, and the Kalman filter separate. We can thus separately design the admittance controller without affecting the overall system stability. Next, we show how the dynamics of the three subsystems separate.

First, consider the quadcopter and the position and attitude controller, described by (9) and (10), (12), respectively. Ignoring the noise vectors we have,

$$\dot{s} = As + Bu + f_E, \quad (20)$$

$$y = Cs, \quad (21)$$

$$u = K_1 \hat{s} + K_2 x_r, \quad (22)$$

where K_1 is the state feedback gain matrix and K_2 multiplies the reference position x_r . Recall that in the steady-state Kalman filter equation (16), the vector $\hat{s}_K = (\hat{s}, \hat{f}_x)$ is the estimate of the augmented state. The augmented matrices are composed as follows:

$$A_K = \begin{bmatrix} A & A_{K_1} \\ 0 & 0 \end{bmatrix}, \quad B_K = \begin{bmatrix} B \\ 0 \end{bmatrix}, \quad (23)$$

$$C_K = \begin{bmatrix} C & 0 \end{bmatrix}, \quad L = \begin{bmatrix} L_1 \\ L_2 \end{bmatrix}, \quad (24)$$

where L is obtained from (17). We can thus rewrite (16) as

$$\begin{bmatrix} \dot{\hat{s}} \\ \dot{\hat{f}}_x \end{bmatrix} = \begin{bmatrix} A - L_1 C & A_{K_1} \\ -L_2 C & 0 \end{bmatrix} \begin{bmatrix} \hat{s} \\ \hat{f}_x \end{bmatrix} + \begin{bmatrix} L_1 \\ L_2 \end{bmatrix} y + \begin{bmatrix} B \\ 0 \end{bmatrix} u. \quad (25)$$

Furthermore, the admittance controller described by (19) can be written as a first-order system with $\xi_r = (x_r, \dot{x}_r)$:

$$\dot{\xi}_r = A_{ad}\xi_r + B_{ad}\hat{f}_x + B_{ad,2}x_d, \quad (26)$$

$$x_r = C_{ad}\xi_r. \quad (27)$$

Defining the full state vector $l = (s, \xi_r, s - \hat{s}, \hat{f})$ leads to the following closed-loop system:

$$\dot{l} = A_{CL}l + B_{CL,1}f_E + B_{CL,2}x_d, \quad (28)$$

with the closed-loop system matrix defined as

$$A_{CL} = \begin{bmatrix} A + BK_1 & BK_2C_{ad} & -BK_1 & 0 \\ 0 & A_{ad} & 0 & -B_{ad} \\ 0 & 0 & A - L_1C & -A_{K_1} \\ 0 & 0 & L_2C & 0 \end{bmatrix}. \quad (29)$$

The eigenvalues of A_{CL} correspond to the eigenvalues of the three diagonal blocks. Thus, the eigenvalues of the closed-loop system are the eigenvalues of the position and attitude controller with perfect state feedback (20)-(22), of the admittance controller (26), and of the Kalman filter (25).

IV. PHYSICAL HUMAN-QUADROPTER INTERACTION

In this section, we explore the possibility of physical human-vehicle interaction by presenting experimental results. We describe the Flying Machine Arena testbed and we provide experimental data for the proposed application of admittance control to quadcopters.

A. Experimental testbed

We demonstrate physical human-robot interaction on small custom quadcopters in the Flying Machine Arena, a 10 x 10 x 10 m testbed for quadcopter research. The quadcopters are equipped with soft propellers that do not seriously harm the user in the event of accidental contact. The space is equipped with a motion capture system that provides vehicle position and attitude measurements. This information is sent to a PC, which runs algorithms and control strategies, and sends commands to the quadcopter at approximately 50 Hz. More details on the testbed can be found in [16].

B. Physical human-quadcopter interaction

1) *Description*: In this experiment, we exploit the ability of admittance control to change the apparent inertia, damping, and stiffness of the robot. When a quadcopter is pushed or pulled (Figure 1), the reference trajectory will accommodate the force exerted by the user behaving as an object of mass 0.5 kg subject to damping (damping coefficient 0.5). Note that the experiment was performed with a quadcopter not carrying a brick.

2) *Controller switching strategy*: If no force is acting on the vehicle, the control scheme presented above simply reduces to the underlying position controller. However, non-idealities (such as propeller efficiency, gyroscope offset) and noise result in non-zero estimated forces. Depending on the choice of the admittance controller parameters, these non-zero forces may cause a slow drift of the reference position. To avoid this, we use the magnitude of the estimated forces to identify when physical interaction with the robot occurs. In position control mode, we monitor the estimated external forces. If forces exceeding a threshold value (0.3 N) are applied to the quadcopter for more than a given time (0.3 seconds), we switch to interaction mode, activating the admittance controller. The converse applies to exit the interaction mode.

3) *Results*: Figure 4 shows the reference trajectory and the actual position of a quadcopter and the estimated external forces along the x and z coordinates during physical interaction with the user. The grey regions indicate when the admittance controller is turned on. It can be seen how the reference trajectory accommodates the external forces acting on the vehicle, which modifies its position accordingly. The lower plot shows the magnitude of the external forces. The chosen switching strategy avoids unnecessary controller changes.

V. CONCLUSIONS

With aerial robots increasingly interacting with their environment, adequate control techniques are necessary. Many strategies have been already investigated and applied to robotic arms and ground robots. In this work, we presented the application of admittance control to a quadcopter. An outer control loop is built on top of an underlying position control, to modify the reference trajectory according to external forces acting on the vehicle. An estimate of these forces is obtained from position and attitude measurements by using an unscented Kalman filter. The closed-loop system is analyzed for a quadcopter near hover, showing that the dynamics of the different subsystems separate.

The framework of admittance control provides an intuitive way for people to physically interact with the vehicle. Indeed, it allows us to define the apparent inertia, damping, and stiffness of the quadcopter subject to forces exerted by the user interacting with it. The presented experimental results have shown the suitability of this method.

In the future, the force/torque estimate can be further improved by using onboard sensors, such as accelerometers and gyroscopes. A hybrid position/force control strategy

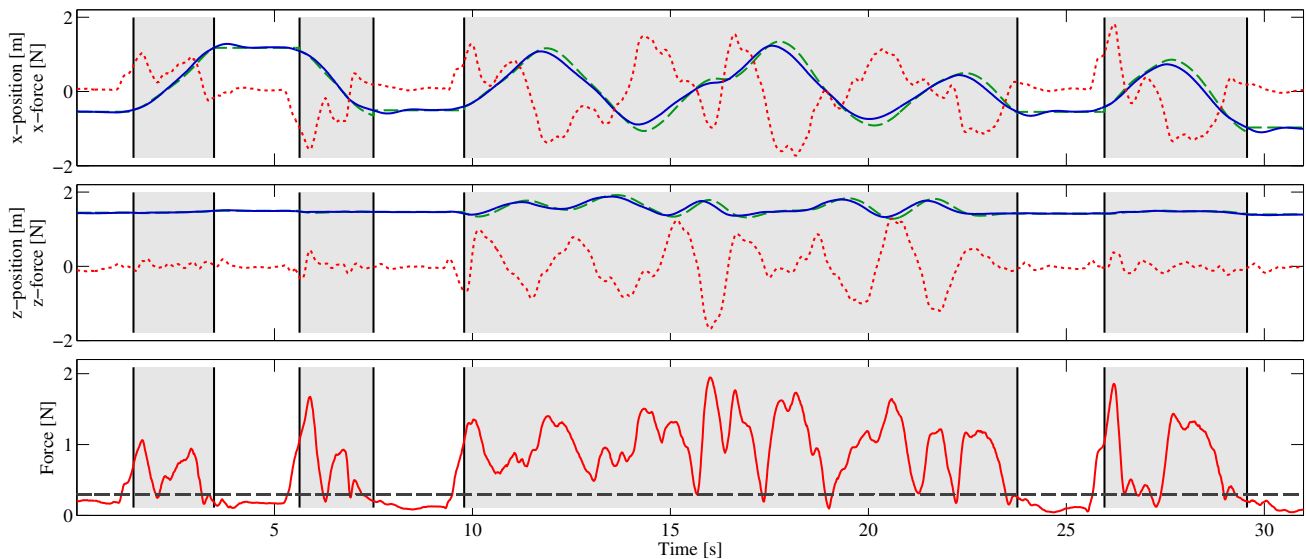


Fig. 4. The trajectory of a quadcopter during physical interaction with a human. The two upper plots show the reference (dashed green) and actual (solid blue) position of a quadcopter and the estimated external force (dotted red) acting on it for the x and z components, respectively. The lower plot indicates the magnitude of the estimated external force acting on the vehicle (solid red) and the threshold value (dashed grey) that controls the switching between admittance controller (grey regions) and position controller (white regions). Note how the combined time/force switching strategy (see Section IV-B.2) avoids unnecessary controller switches during the interaction phases.

exploiting admittance control could also be investigated and compared to existing results for UAVs.

ACKNOWLEDGMENTS

This paper builds on the work of many members of the Flying Machine Arena; a complete list of contributions can be found online [14]. The authors especially thank Mark W. Mueller for his contributions to the force estimator.

This work was supported by the Hartmann Müller-Fonds on ETH Research Grant ETH-30 12-1.

REFERENCES

- [1] L. Meier, P. Tanskanen, F. Fraundorfer, and M. Pollefeys, "PIXHAWK: A system for autonomous flight using onboard computer vision," in *IEEE International Conference on Robotics and Automation*, 2011, pp. 2992–2997.
- [2] R. Mahony, V. Kumar, and P. Corke, "Multirotor Aerial Vehicles: Modeling, Estimation, and Control of Quadrotor," *IEEE Robotics & Automation Magazine*, vol. 19, no. 3, pp. 20–32, Sep. 2012.
- [3] N. Michael, J. Fink, and V. Kumar, "Cooperative manipulation and transportation with aerial robots," *Autonomous Robots*, vol. 30, no. 1, pp. 73–86, Sep. 2010.
- [4] M. Bernard, K. Kondak, I. Maza, and A. Ollero, "Autonomous transportation and deployment with aerial robots for search and rescue missions," *Journal of Field Robotics*, vol. 28, no. 6, pp. 914–931, 2011.
- [5] D. Mellinger, Q. Lindsey, M. Shomin, and V. Kumar, "Design, modeling, estimation and control for aerial grasping and manipulation," in *IEEE/RSJ International Conference on Intelligent Robots and Systems*, 2011, pp. 2668–2673.
- [6] V. Parra-Vega, A. Sanchez, C. Izaguirre, O. Garcia, and F. Ruiz-Sanchez, "Toward Aerial Grasping and Manipulation with Multiple UAVs," *Journal of Intelligent & Robotic Systems*, vol. 70, pp. 575–593, 2013.
- [7] P. E. I. Pounds, D. R. Bersak, and A. M. Dollar, "Stability of small-scale UAV helicopters and quadrotors with added payload mass under PID control," *Autonomous Robots*, vol. 33, no. 1-2, pp. 129–142, 2012.
- [8] "AIRobots." [Online]. Available: <http://www.airrobots.eu>
- [9] L. Marconi and R. Naldi, "Control of Aerial Robots: Hybrid Force and Position Feedback for a Ducted Fan," *IEEE Control Systems*, vol. 32, no. 4, pp. 43–65, 2012.
- [10] S. Bellens, J. De Schutter, and H. Bruyninckx, "A hybrid pose / wrench control framework for quadrotor helicopters," in *IEEE International Conference on Robotics and Automation*, 2012, pp. 2269–2274.
- [11] F. Forte and R. Naldi, "Impedance control of an aerial manipulator," *American Control Conference*, pp. 3839–3844, 2012.
- [12] "Integrated Project Aerial Robotics Cooperative Assembly System." [Online]. Available: <http://www.arcas-project.eu/>
- [13] M. Orsag, C. Korpela, and P. Oh, "Modeling and Control of MM-UAV: Mobile Manipulating Unmanned Aerial Vehicle," *Journal of Intelligent & Robotic Systems*, vol. 69, pp. 227–240, 2013.
- [14] "Flying Machine Arena." [Online]. Available: <http://www.flyingmachinearena.org>
- [15] "Qball-X4, Quanser." [Online]. Available: http://quanser.com/english/html/UVS_Lab/fs_Qball_X4.htm
- [16] S. Lupashin, A. P. Schoellig, M. Hehn, and R. D'Andrea, "The Flying Machine Arena as of 2010," in *IEEE International Conference on Robotics and Automation*, 2011, pp. 2970–2971.
- [17] N. Hogan, "Impedance Control: An Approach to Manipulation," in *American Control Conference*, 1984, pp. 304–313.
- [18] M. W. Spong, S. Hutchinson, and M. Vidyasagar, *Robot Modeling and Control*. Wiley, 2005.
- [19] A. P. Schoellig, C. Wiltche, and R. D'Andrea, "Feed-forward parameter identification for precise periodic quadcopter motions," in *American Control Conference*, 2012, pp. 4313–4318.
- [20] L. Villani and J. De Schutter, "Force Control," in *Springer Handbook of Robotics*, B. Siciliano and O. Khatib, Eds. Berlin Heidelberg: Springer-Verlag, 2008, pp. 161–185.
- [21] AIRobots, "Human-UAV Interaction," 2012. [Online]. Available: <http://youtu.be/R4hdHwbCDac>
- [22] J. Willmann, F. Augugliaro, T. Cadalbert, R. D'Andrea, F. Gramazio, and M. Kohler, "Aerial Robotic Construction Towards a New Field of Architectural Research," *International Journal of Architectural Computing*, vol. 10, no. 3, pp. 439–460, 2012.
- [23] M. Hehn and R. D'Andrea, "Quadcopter Trajectory Generation and Control," in *IFAC World Congress*, 2011, pp. 1485–1491.
- [24] S. Julier and J. Uhlmann, "Unscented Filtering and Nonlinear Estimation," *Proceedings of the IEEE*, vol. 92, no. 3, pp. 401–422, 2004.
- [25] D. Simon, *Optimal State Estimation: Kalman, H Infinity, and Nonlinear Approaches*. John Wiley & Sons, 2006.